THE JOURNAL OF PHYSICAL CHEMISTRY C
A JOURNAL OF THE AMERICAN CHEMICAL SOCIETY

pubs.acs.org/JPCC

Article

Novel Prediction Model of Band Gap in Organic–Inorganic Hybrid Perovskites Based on a Simple Cluster Model Database

Zhengyang Gao, Yang Bai, Min Wang, Guangyang Mao, Xiaoshuo Liu, Peng Gao, Weijie Yang, Xunlei Ding,* and Jianxi Yao

Cite This: *J. Phys. Chem. C* 2022, 126, 13409–13415

Read Online

ACCESS | Metrics & More | Article Recommendations | Supporting Information

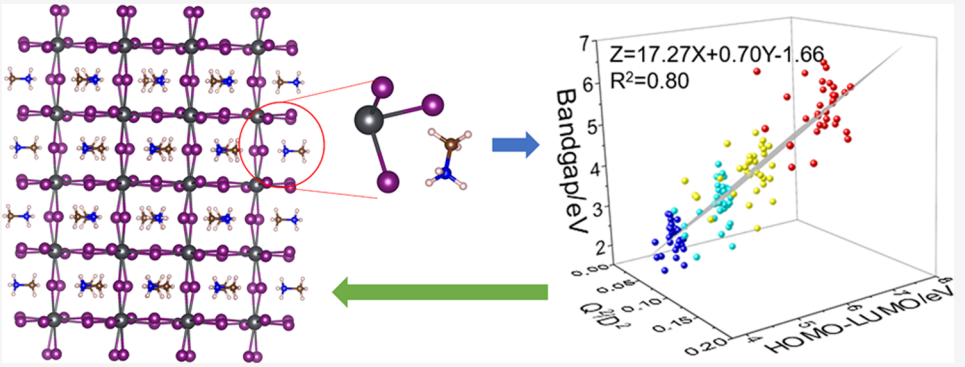

ABSTRACT: Organic–inorganic hybrid perovskite materials with high photoelectric conversion efficiency are currently the most promising materials in the development of new-generation solar cells. It is quite easy to calculate the highest occupied molecular orbital–lowest unoccupied molecular orbital (HOMO–LUMO) gap of a cluster, while it is difficult to calculate the band gap of bulk materials accurately. Therefore, in this work, we constructed a cluster model database with 352 ABX_3 structures (A = monovalent cations, B = divalent cations, and X = monovalent anions). Based on the properties of the cluster models, including the HOMO–LUMO gap, the charges on A^+, and the distance of H...X (H atoms are in A^+), a valid prediction model was proposed for the band gap of bulk materials with the coefficient of determination R^2 = 0.80. Based on this model, we found several new perovskites with suitable band gaps, which may guide the exploitation and development of new materials.

1. INTRODUCTION

In recent years, organic–inorganic hybrid perovskites, often denoted as ABX_3 (generally, A = monovalent cations, B = divalent metal cations, and X = monovalent anions), have developed rapidly for the high photoelectric conversion efficiency.[1−8] At present, the efficiency of similar materials has topped over 25%,[9] which is comparable to single-crystal silicon materials.

In previous studies on perovskites,[10−16] the cluster model has shown a lot of advantages because of the small calculation cost, while the periodic structures have a huge cost in calculations for the band gap, which is the essential property for photoelectric conversion as well as other important parameters of the materials. Although the highest occupied molecular orbital–lowest unoccupied molecular orbital (HOMO–LUMO) gap and the band gap have a close relationship from the point of view of electronic structures, the calculated values based on density functional theory (DFT) are quite different for them. Taking $MAPbI_3$ ($CH_3NH_3PbI_3$) as an example, the band gap of the periodic model is about 1.53 eV[17] with the high-precision hybrid functional Heyd–Scuseria–Ernzerh (HSE). As for the cluster models, some researchers calculated the HOMO–LUMO gap of $MAPbI_3$ with different methods, including coupled cluster single double (triple) (CCSD(T)) (9.23 eV),[14] time-dependent DFT with Becke three-parameter Lee–Yang–Parr functionals (B3LYP) (4.5 eV),[14] B3LYP (4.67 eV),[18] and M06-2X (3.67 eV).[11] Unfortunately, the calculation results of the cluster models above are far from the periodic models, and the difference may be caused by both calculation models and methods. Therefore, the inaccurate prediction of band gap of perovskites based on the HOMO–LUMO gaps of cluster models makes it difficult for most scholars to be convinced, and the applications of cluster models in perovskite research were limited. To solve this problem, some researchers have proposed several methods to improve the accuracy of the

Received: May 2, 2022
Revised: July 19, 2022
Published: July 28, 2022

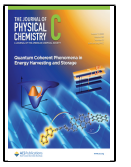

https://doi.org/10.1021/acs.jpcc.2c03016
J. Phys. Chem. C 2022, 126, 13409–13415

cluster models. Giorgi et al.[18] constructed several cluster structures by an increasing number of Pb atoms with the same number of octahedrons. The calculation results are 4.67, 4.23, 3.70, and 3.50 eV for 1, 2, 8, and 12 octahedrons, respectively. We can find that with the increasing number of calculation units, the HOMO−LUMO gap of the cluster models gradually decreases and moves closer to the results of the periodic models. However, the calculation accuracy still cannot reach the band gap calculated by the periodic models at the HSE level. Furthermore, this complicated modeling method needs to construct a series of cluster models and perform DFT calculations on all of these clusters, which is quite time-consuming. Therefore, it is important to find a new way to predict the band gap of bulk perovskites based on calculations with simple cluster models. Considering the close relationship between the two types of gaps, it is also essential that the prediction model is based on the HOMO−LUMO gap of clusters.

In this work, we performed three main tasks. First, we constructed a cluster model database with a scale of 352 cluster structures based on DFT calculations (Table S1). Second, we proposed a prediction model for the band gap of bulk materials with the coefficient of determination R^2 = 0.80 based on the properties of cluster models, which provides a deep understanding based on the relationship between the cluster models and the periodic models. Third, we predicted several promising systems with suitable band gaps.

2. CALCULATION METHODS

DFT has been used for its high accuracy and relatively low computational cost. The Gaussian 09 software package[19] was used to perform DFT calculations with the cluster model of perovskites. B3LYP hybrid functional[20] and def2SVP basis sets[21,22] were used in the DFT calculations, and Grimme's DFT-D3 method[23] was used for corrections of dispersion interactions. All of the cluster structures were optimized to have the minimal energy with the neutral charge state.

The cluster models are actually the smallest structure units, ABX_3, which were derived from the periodic models of bulk perovskite materials. Theoretical calculations on materials can provide a large amount of data without influences of experimental synthesis conditions. The periodic structures and data involved in this research come from an open-source database[24] based on DFT calculations with the HSE hybrid functional. In this database, each perovskite generally has several different configurations, including three-dimensional (3D) structures, two-dimensional (2D) planner structures, and 2D pillar structures. Data of 3D structures were selected as the fitting object in this work (except $EASnBr_3$ with data only for 2D structures), and the average band gap values of the 3D structures were used for each ABX_3.

In the model validation part, periodic structures were constructed to calculate the band gap. We carry out first-principles calculations using the Vienna ab initio simulation package (VASP)[25,26] with the projector augmented wave (PAW) formalism.[27] The HSE hybrid functional[28] was used with the plane-wave cutoff energy of 520 eV. The ions were relaxed until the maximum force on each atom was smaller than 0.02 eV $Å^{-1}$, and the total energy was obtained when it converged to 10^{-5} eV in the electronic self-consistent loop. Grimme's DFT-D3 corrections were also included through setting IVDW = 12. A 2 × 6 × 6 γ-centered K-point grid was used during the calculations.

3. RESULTS AND DISCUSSION

3.1. Cluster Model Database. In this work, a cluster model database was constructed with a scale of 352 cluster structures. Figure 1a−h shows the typical cluster structures of

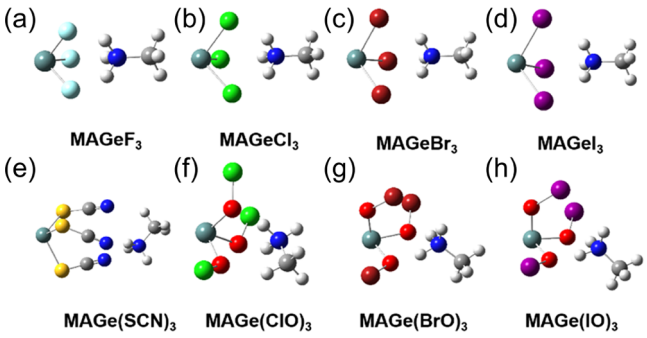

Figure 1. Typical cluster structures for $MAGeX_3$ (X = F, Cl, Br, I, SCN, ClO, BrO, and IO in panels (a−h), respectively).

$MAGeX_3$ as an example. The geometric structures of other perovskite materials are similar to the structures mentioned above. In the database, 11 types of A^+ sites were MA^+ = $CH_3NH_3^+$, FA^+ = $NH_2CHNH_2^+$, LA^+ = $(CH_3)_2NH_2^+$, TA^+ = $(CH_3)_2CHNH_3^+$, RA^+ = $C_3N_2H_5^+$, EA^+ = NH_3OH^+, UA^+ = $(CH_3)_3NH^+$, DA^+ = $(CH_3)_4N^+$, KA^+ = $CH_3CH_2NH_3^+$, KB^+ = $CH_3CH_2CH_2NH_3^+$, and KC^+ = $CH_3CH_2CH_2CH_2NH_3^+$, four types of B^{2+} sites were Ge^{2+}, Sn^{2+}, Pb^{2+}, and Zn^{2+}, and eight types of X^- sites were F^-, Cl^-, Br^-, I^-, SCN^-, ClO^-, BrO^-, and IO^-. The electron affinity of pseudo-halide ions (e.g., SCN^-) is similar to halide ions, so it is reasonable to construct new perovskites by replacing halide ions with pseudo-halide ions.[29] Properties of these cluster structures are listed in Table S1, including the HOMO−LUMO gap, the molecular volume, the charge on A^+, the ionization energy of ABX_3, binding energy of $A^+...BX_3^-$, and the shortest distance of H...X (the H atoms in A^+).

Among these organic cationic groups and anionic groups, MA^+ and the halide groups (F^-, Cl^-, Br^-, and I^-) were the most popular, and these types of perovskite materials have been widely investigated. Table 1 shows the calculated results for two geometric parameters, the shortest distance of H...X (D, Å) (the H atoms in A^+) and the shortest bond length of B−X (R_1, Å) of $MABX_3$. Data from refs 14, 30, and 31 are for

Table 1. Calculated Results of the Shortest Distance of H...X (D, Å) and the Shortest Bond Lengths of B−X (R_1, Å) Compared with those in Previous Studies

ABX_3	D	R_1
$MAGeF_3$	1.72	1.87
$MAGeCl_3$	2.18	2.37 (2.33)[34] (2.39)[29]
$MAGeBr_3$	2.33	2.54 (2.53)[30]
$MAGeI_3$	2.53	2.77 (2.77)[30] (2.78)[33]
$MASnF_3$	1.68 (1.78)[31]	2.06
$MASnCl_3$	2.17 (2.21)[31]	2.55 (2.57)[14] (2.60)[29]
$MASnBr_3$	2.33 (2.36)[31]	2.72 (2.72)[14] (2.69)[29]
$MASnI_3$	2.54 (2.56)[31]	2.94 (2.99)[14]
$MAPbF_3$	1.66 (1.75)[31]	2.16
$MAPbCl_3$	2.16 (2.20)[31] (2.12)[32]	2.64 (2.66)[14] (2.72)[29]
$MAPbBr_3$	2.32 (2.36)[31] (2.33)[32]	2.80 (2.83)[14] (2.97)[34]
$MAPbI_3$	2.54 (2.56)[31] (2.52)[32]	3.02 (3.04)[14]

https://doi.org/10.1021/acs.jpcc.2c03016
J. Phys. Chem. C 2022, 126, 13409−13415

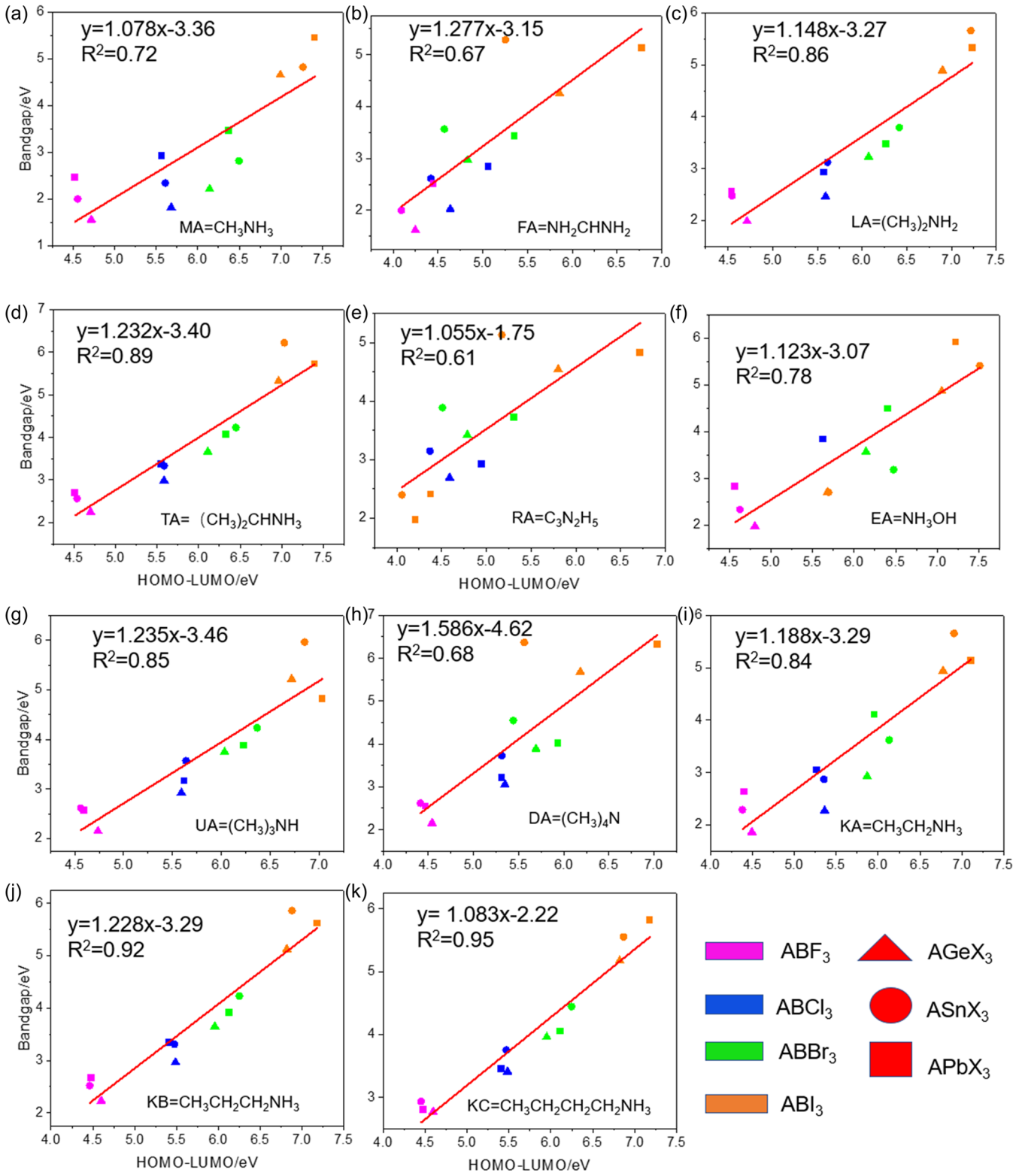

Figure 2. Linear relationship between the HOMO−LUMO gap of the cluster models and the band gap of the periodic models for ABX_3 with different types of A^+ cations (a−k). The purple, blue, green, and orange points denote systems with X = F, Cl, Br, and I, respectively, while the triangle, circle, and square points represent B = Ge, Sn, and Pb, respectively.

cluster models and data from refs 29 and 32−34 are for periodic models. The results in this work are very close to those in previous studies with difference less than 5% for most cases, indicating that the cluster models and the calculation methods in this work are reliable.

3.2. Prediction Models Based on Properties of Cluster Models. The band gap of photoelectric materials has a great impact on the optical properties of the perovskite materials. The light absorption efficiency of perovskite materials will be reduced if the gap is too large or too small. Hence, it is a

https://doi.org/10.1021/acs.jpcc.2c03016
J. Phys. Chem. C 2022, 126, 13409−13415

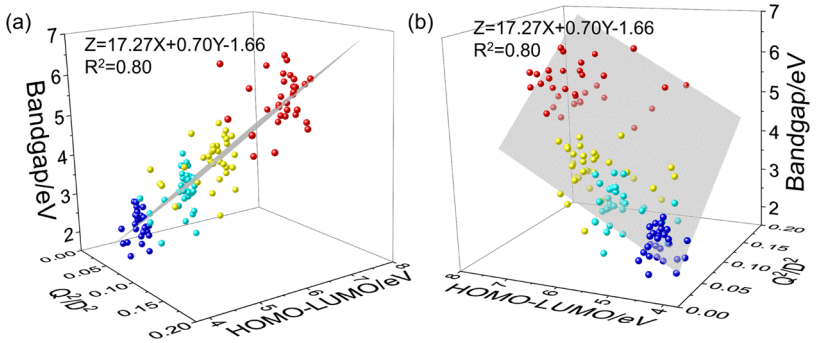

Figure 3. Side (a) and top (b) views of the plane relationship of Q^2/D^2 and HOMO−LUMO gaps of cluster models and the band gap of periodic models. The purple, blue, yellow, and red points denote ABX_3 with X = F, Cl, Br, and I, respectively.

feasible method to select perovskite materials according to the band gap, which can be obtained accurately by periodic models. Due to the lack of data for bulk materials with Zn^{2+}, SCN^-, ClO^-, BrO^-, and IO^-, only 132 structures are chosen to explore the relationship between the HOMO−LUMO gap of the cluster models and the band gap of the periodic models, including 11 types of A^+, three types of B^{2+}, and four types of halogen anions (Figure 2).

Figure 2a−k shows the linear fitting of the HOMO−LUMO gap and the band gap for different types of A^+. For every type of A^+, the two gaps have a similar increased relationship with the sequential increase of the atomic number of halogen ions. The reason for this trend is the decrease of electronegativity of the halogen ions from F to I. Although the situations of systems with different A^+ cations are not precisely consistent, the overall trend is the same, which can also prove the rationality of the cluster models. It is noticeable that a number of them showed a nice linear relationship with the values of R^2 over 0.80, such as (LA^+, TA^+, UA^+, KA^+, KB^+, KC^+), while the rest of the structures showed a poor linear relationship with values of R^2 between 0.6 and 0.8. The linear fitting with all 132 systems together was also performed, as shown in Figure S1. The overall trend is maintained while R^2 is also not high (0.66).

To weaken the influence caused by the different A^+ sites in different systems and to obtain a general relationship that can precisely adapt to more systems, additional properties are needed to consider for revising the linear relationship of the HOMO−LUMO gap of the cluster models and the band gap of the periodic models. By comparing the relationship between the individual variables in the database and the HOMO−LUMO gap, we found that Q and D have remarkable effects on the HOMO−LUMO gap of the clusters in which Q represents the Hirshfeld charge on the A^+ organic cation, and D represents the shortest distance of H...X (H atoms are in A^+). Q reflects the process of charge transfer, which changes the electron distribution not only among atoms but also in molecular orbitals and thus may have a close relationship with the band gap of bulk materials. A smaller D represents a stronger binding ability between A^+ and BX_3^- parts and a higher possibility for the orbital overlap between H in A^+ and X and thus also affects the band gap significantly. Therefore, Q and D can provide some microscopic electronic and geometric structure information and thus can be used to revise the fitting relationship between the HOMO−LUMO gap of the cluster models and the band gap of the periodic models. We tried a variety of combination functions of Q and D and take them and the HOMO−LUMO gap as two variables to conduct two-dimensional linear fitting (plane fitting) for the band gap of bulk materials. With the plane relationship, a new descriptive variable Q^2/D^2 was proposed, which is just the expression of the Coulombic interaction force between A^+ and BX_3^- and thus can reflect the interaction strength of the two parts, as shown in Figure 3a,b.

With the new descriptive variable, the fitting plane equation was established

$$Z = 17.27X + 0.70Y - 1.66 \quad (1)$$

with $R^2 = 0.80$. In this equation, X, Y, and Z are Q^2/D^2, the HOMO−LUMO gap, and band gap, respectively. Using this equation, the band gap of new perovskite materials can be predicted after obtaining the HOMO−LUMO gap and the Q^2/D^2 value of the cluster model. It takes less time for modeling and optimizing with cluster models, which is difficult to achieve in periodic models or experiment preparation.

At present, it is recognized that materials with high photoelectric performance should have a band gap of about 1.6 eV according to experimental measurements.[35] It is proper to select potential perovskite materials according to this value. It should be pointed out that the band gap database[24] used in this work was based on DFT calculations with HSE hybrid functional, which may be quite reliable for most cases, while it was also found that the computed band gap by DFT may differ from the experimental values significantly in other cases. Therefore, an acceptable range of the band gap (Z) was set as 1.6 ± 0.4 eV. That is, the upper and lower limits are 1.2 and 2.0 eV, respectively. Accordingly, the fitting eq 1 obtained above can be modified, and a new inequality was obtained

$$2.86 < 17.27X + 0.70Y < 3.66 \quad (2)$$

which can be used directly to select promising materials.

Our cluster model database includes 352 structures, and data of 132 clusters were used to obtain the above equation with known data of bulk materials. The rest 220 clusters were screened with inequality 2, as shown in Figure 4. Most of these clusters are with X = ClO, BrO, IO, SCN. In Figure 4, two green lines represent the upper and lower limits, and 13 promising structures were initially shown up. They are $EAGe(IO)_3$, $EAPb(IO)_3$, $EASn(IO)_3$, $EAZn(IO)_3$, $TAGe(IO)_3$, $TAPb(IO)_3$, $TAZn(IO)_3$, $TASn(IO)_3$, $KASn(IO)_3$, $KAPb(IO)_3$, $KAZn(IO)_3$, $KbPb(IO)_3$, and $KCPb(IO)_3$. According to the prediction in Figure 4, most materials may have too large band gaps, except the ones with IO^- and various A^+ organic cations, which are rarely studied. The IO^- ion has similar chemical properties with the halide ion I^-. The ionic radius of IO^- is 2.0 Å,[36] which is close to that of I^- (2.1 Å).

https://doi.org/10.1021/acs.jpcc.2c03016
J. Phys. Chem. C 2022, 126, 13409−13415

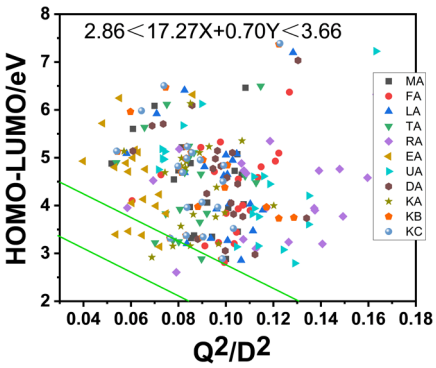

Figure 4. Prediction of promising systems to have suitable band gaps.

Small vertical ionization energy (VDE) of I^- (3.30 eV)[36] corresponds to a weaker holding capability of the valence electron in BX_3^-. This suggests a lower bonding ionicity and smaller band gap of $MAPbI_3$. IO^- has an even lower VDE (2.46 eV),[36] which may lead to small band gaps of IO^--containing materials. In a previous work,[36] with partial replacement of I^- by IO^- in $MAPbI_3$, $MAPbI_{2.75}(IO)_{0.25}$ was predicted to have good water-resistant properties through theoretical calculations.

3.3. Model Validation. In the 13 promising systems that may have suitable band gap for photoelectric conversion, some of them are selected to verify the rationality of our work. Lead-containing perovskites are not selected due to their possible toxicity. TA-containing ones are not selected because TA is too large and a lot of time will be cost. Furthermore, Zn shows a different valence structure from Ge, Sn, and Pb, and so the Zn-containing ones are also not selected. Thus, only three system, $EAGe(IO)_3$, $EASn(IO)_3$, and $KASn(IO)_3$, are selected to construct periodic structures and calculate band gaps.

Orthorhombic crystal structures were built for three systems, and the optimized structures are shown in Figure S2a–c. Then, band structures were calculated with HSE functional and shown in Figure S3a–c. The band gaps obtained are 1.38, 1.30, and 1.52 eV for $EAGe(IO)_3$, $EASn(IO)_3$, and $KASn(IO)_3$, respectively. These band gap values are in the ideal range (1.2–2.0 eV), indicating that three materials may have outstanding photoelectric conversion performance. It also demonstrates that the prediction ability of our cluster models is acceptable. Note that the raw data taken from the band gap database were obtained by DFT calculations, and the above band gap values of the three materials are also calculated data. Thus, it is essential to perform further experiments to confirm their high performance of photoelectric conversion.

4. CONCLUSIONS

In this work, a cluster model database containing 11 types of A^+, four types of B^{2+}, and eight types of X^- was established based on density functional theory. The linear fitting relationship and plane fitting relationship between the cluster models and the periodic models were performed. Among them, the coefficient of determination (R^2) of the plane fitting relationship between the band gap of bulk perovskite materials and (HOMO–LUMO gap, Q^2/D^2) of cluster models is 0.80. We propose a practical prediction model of band gap of organic–inorganic hybrid perovskites based on a simple cluster model database based on which several promising photoelectric materials are suggested with suitable band gaps. Therefore, our work is stimulating that may guide the preparation of new perovskite materials in future work.

■ ASSOCIATED CONTENT

Supporting Information

The Supporting Information is available free of charge at https://pubs.acs.org/doi/10.1021/acs.jpcc.2c03016.

Detailed data of the cluster model database; the linear fitting with all 132 clusters together, and more properties of the three predicted materials (PDF)

■ AUTHOR INFORMATION

Corresponding Author

Xunlei Ding − *School of Mathematics and Physics and Institute of Clusters and Low Dimensional Nanomaterials, School of Mathematics and Physics, North China Electric Power University, Beijing 102206, China; Hebei Key Laboratory of Physics and Energy Technology, North China Electric Power University, Baoding 071000, China;* orcid.org/0000-0002-9962-714X; Email: dingxl@ncepu.edu.cn

Authors

Zhengyang Gao − *Department of Power Engineering, School of Energy, Power, and Mechanical Engineering, North China Electric Power University, Baoding 071000, China*

Yang Bai − *Department of Power Engineering, School of Energy, Power, and Mechanical Engineering, North China Electric Power University, Baoding 071000, China*

Min Wang − *Department of Power Engineering, School of Energy, Power, and Mechanical Engineering, North China Electric Power University, Baoding 071000, China*

Guangyang Mao − *Department of Power Engineering, School of Energy, Power, and Mechanical Engineering, North China Electric Power University, Baoding 071000, China*

Xiaoshuo Liu − *Department of Power Engineering, School of Energy, Power, and Mechanical Engineering, North China Electric Power University, Baoding 071000, China; Key Laboratory of Energy Thermal Conversion and Control of Ministry of Education, School of Energy and Environment, Southeast University, Nanjing 210096, China*

Peng Gao − *Department of Power Engineering, School of Energy, Power, and Mechanical Engineering, North China Electric Power University, Baoding 071000, China*

Weijie Yang − *Department of Power Engineering, School of Energy, Power, and Mechanical Engineering, North China Electric Power University, Baoding 071000, China;* orcid.org/0000-0002-0232-1129

Jianxi Yao − *State Key Laboratory of Alternate Electrical Power System With Renewable Energy Sources and Beijing Key Laboratory of Energy Safety and Clean Utilization, North China Electric Power University, Beijing 102206, China;* orcid.org/0000-0002-5472-9337

Complete contact information is available at: https://pubs.acs.org/10.1021/acs.jpcc.2c03016

Author Contributions

Z.G.: project administration, software. Y.B.: writing—original draft, investigation, data curation, visualization. M.W.: formal analysis, investigation. G..M.: investigation. X.L.: writing—review & editing. P.G.: supervision. W.Y.: writing—review & editing, conceptualization, project administration. X.D.: project

https://doi.org/10.1021/acs.jpcc.2c03016
J. Phys. Chem. C 2022, 126, 13409−13415

administration, writing—review & editing, software. J.Y.: project administration, funding acquisition.

Notes

The authors declare no competing financial interest.

The data used or analyzed during the current study are available on reasonable request.

■ ACKNOWLEDGMENTS

This work was supported by the National Natural Science Foundation of China (92161115, 61704054), the National Key Research and Development Program of China (No. 2016YFA0202401), and the Fundamental Research Fund for the Central Universities (JB2015RCY03, JB2019MS052, JB2017MS056). The work was also supported by the Beijing Natural Science Foundation (No. 2214064).

■ REFERENCES

(1) Park, N. G. Organometal Perovskite Light Absorbers Toward a 20% Efficiency Low-Cost Solid-State Mesoscopic Solar Cell. *J. Phys. Chem. Lett.* **2013**, *4*, 2423−2429.

(2) Im, J. H.; Lee, C. R.; Lee, J. W.; Park, S. W.; Park, N. G. 6.5% Efficient Perovskite Quantum-Dot-Sensitized Solar Cell. *Nanoscale* **2011**, *3*, 4088−4093.

(3) Service, R. F. Perovskite Solar Cells Keep on Surging. *Science* **2014**, *344*, No. 458.

(4) Jeon, N. J.; Na, H.; Jung, E. H.; Yang, T. Y.; Lee, Y. G.; Kim, G.; Shin, H. W.; Seok, S. Il.; Lee, J.; Seo, J. A Fluorene-Terminated Hole-Transporting Material for Highly Efficient and Stable Perovskite Solar Cells. *Nat. Energy* **2018**, *3*, 682−689.

(5) Service, R. F. Perovskite Solar Cells Gear Up to Go Commercial. *Science* **2016**, *354*, 1214−1215.

(6) Kojima, A.; Teshima, K.; Shirai, Y.; Miyasaka, T. Organometal Halide Perovskites as Visible-Light Sensitizers for Photovoltaic Cells. *J. Am. Chem. Soc.* **2009**, *131*, 6050−6051.

(7) Li, Z.; Gao, Y.; Zhang, Z.; Xiong, Q.; Deng, L.; Li, X.; Zhou, Q.; Fang, Y.; Gao, P. PCN-Regulated SnO_2 Composites Enables Perovskite Solar Cell with Efficiency Beyond 23%. *Nano-Micro Lett.* **2021**, *13*, No. 101.

(8) Gao, Z.; Wang, W.; Zhang, H.; Chen, S.; Wu, C.; Gates, I. D.; Yang, W.; Ding, X.; Yao, J. Design of $(C_3N_2H_5)_{1-x}Cs_xPbI_3$ as a Novel Hybrid Perovskite With Strong Stability and Excellent Photoelectric Performance: A Theoretical Prediction. *Sol. Energy Mater. Sol. Cells* **2021**, *233*, No. 111401.

(9) Yoo, J. J.; Seo, G.; Chua, M. R.; Park, T. G.; Lu, Y.; Rotermund, F.; Kim, Y. K.; Moon, C. S.; Jeon, N. J.; Correa-Baena, J. P.; et al. Efficient Perovskite Solar Cells via Improved Carrier Management. *Nature* **2021**, *590*, 587−593.

(10) Gao, Z.; Chen, S.; Bai, Y.; Wang, M.; Liu, X.; Yang, W.; Li, W.; Ding, X.; Yao, J. A New Perspective for Evaluating the Photoelectric Performance of Organic-Inorganic Hybrid Perovskites Based on the DFT Calculations of Excited States. *Phys. Chem. Chem. Phys.* **2021**, *23*, 11548−11556.

(11) Varadwaj, A.; Varadwaj, P. R.; Yamashita, K. Revealing the Cooperative Chemistry of the Organic Cation in the Methylammonium Lead Triiodide Perovskite Semiconductor System. *ChemistrySelect* **2018**, *3*, 7269−7282.

(12) Neukirch, A. J.; Abate, I. I.; Zhou, L.; Nie, W.; Tsai, H.; Pedesseau, L.; Even, J.; Crochet, J. J.; Mohite, A. D.; Katan, C.; Tretiak, S. Geometry Distortion and Small Polaron Binding Energy Changes With Ionic Substitution in Halide Perovskites. *J. Phys. Chem. Lett.* **2018**, *9*, 7130−7136.

(13) Alkorta, I.; Elguero, J. A Theoretical Study of Perovskites Related To $CH_3NH_3PbX_3$ (X = F, Cl, Br, I). *New J. Chem.* **2018**, *42*, 13889−13898.

(14) Fang, H.; Jena, P. Molecular Origin of Properties of Organic-Inorganic Hybrid Perovskites: The Big Picture from Small Clusters. *J. Phys. Chem. Lett.* **2016**, *7*, 1596−1603.

(15) De Angelis, F.; Kamat, P. V. Riding the New Wave of Perovskites. *ACS Energy Lett.* **2017**, *2*, 922−923.

(16) Kieslich, G.; Sun, S.; Cheetham, A. K. Solid-State Principles Applied to Organic−Inorganic Perovskites: New Tricks for an Old Dog. *Chem. Sci.* **2014**, *5*, 4712−4715.

(17) Xing, G.; Mathews, N.; Sun, S.; Lim, S. S.; Lam, Y. M.; Gratzel, M.; Mhaisalkar, S.; Sum, T. C. Long-Range Balanced Electron-Transport and Hole-Transport Lengths in Organic-Inorganic $CH_3NH_3PbI_3$. *Science* **2013**, *342*, 344−347.

(18) Giorgi, G.; Yoshihara, T.; Yamashita, K. Structural and Electronic Features of Small Hybrid Organic-Inorganic Halide Perovskite Clusters: A Theoretical Analysis. *Phys. Chem. Chem. Phys.* **2016**, *18*, 27124−27132.

(19) Frisch, M. J.; Trucks, G. W.; Schlegel, H. B.; Scuseria, G. E.; Robb, M. A.; Cheeseman, J. R.; Scalmani, G.; Barone, V.; Petersson, G. A.; Nakatsuji, H. F.et al. *Gaussian 09*, Revision D.01; Gaussian, Inc.: Wallingford CT, 2009.

(20) Stephens, P. J.; Devlin, F. J.; Chabalowski, C. F.; Frisch, M. J. Ab initio calculation of Vibrational Absorption and Circular Dichroism Spectra Using Density Functional Force Fields. *J. Phys. Chem. A* **1994**, *98*, 11623−11627.

(21) Maharjan, P. P.; Chen, Q.; Zhang, L.; Adebanjo, O.; Adhikari, N.; Venkatesan, S.; Adhikary, P.; Vaagensmith, B.; Qiao, Q. Photovoltaic Devices and Characterization of a Dodecyloxybenzothiadiazole-Based Copolymer. *Phys. Chem. Chem. Phys.* **2013**, *15*, 6856−6863.

(22) Weigend, F.; Ahlrichs, R. Balanced Basis Sets of Split Valence, Triple Zeta Valence and Quadruple Zeta Valence Quality For H to Rn: Design and Assessment of Accuracy. *Phys. Chem. Chem. Phys.* **2005**, *7*, 3297−3305.

(23) Kruse, H.; Grimme, S. A Geometrical Correction for the Inter- And Intra-Molecular Basis Set Superposition Error in Hartree-Fock and Density Functional Theory Calculations for Large Systems. *J. Chem. Phys.* **2012**, *136*, No. 154101.

(24) Kim, C.; Huan, T. D.; Krishnan, S.; Ramprasad, R. A Hybrid Organic-Inorganic Perovskite Dataset. *Sci. Data* **2017**, *4*, No. 170057.

(25) Kresse, G.; Furthmüller, J. Efficiency of Ab-Initio Total Energy Calculations for Metals and Semiconductors Using a Plane-Wave Basis Set. *Comput. Mater. Sci.* **1996**, *6*, 15−50.

(26) Kresse, G.; Furthmüller, J. Efficient Iterative Schemes for Ab Initio Total-Energy Calculations Using a Plane-Wave Basis Set. *Phys. Rev. B* **1996**, *54*, 11169−11186.

(27) Neukirch, A. J.; Nie, W.; Blancon, J. C.; Appavoo, K.; Tsai, H.; Sfeir, M. Y.; Katan, C.; Pedesseau, L.; Evrn, J.; Crochet, J. J.; et al. Polaron Stabilization by Cooperative Lattice Distortion and Cation Rotations in Hybrid Perovskite Materials. *Nano Lett.* **2016**, *16*, 3809−3816.

(28) Henderson, T. M.; Paier, J.; Scuseria, G. E. Accurate Treatment of Solids With the HSE Screened Hybrid. *Phys. Status Solidi B* **2011**, *248*, 767−774.

(29) Katan, C.; Pedesseau, L.; Kepenekian, M.; Rolland, A.; Even, J. Interplay of Spin−Orbit Coupling and Lattice Distortion in Metal Substituted 3D Tri-Chloride Hybrid Perovskites. *J. Mater. Chem. A* **2015**, *3*, 9232−9240.

(30) Wang, M.; Li, W.; Lu, F.; Ding, X. Theoretical Study on the Stability of the Complexes ABX_3 [A = $CH_3NH_3^+$, $NH_2CHNH_2^+$, NH_2CHOH^+; B = Sn^{2+}, Pb^{2+}; X = F^-, Cl^-, Br^-, I^-]. *J. Mol. Model.* **2020**, *26*, No. 46.

(31) Fang, H.; Jena, P. Li-Rich Antiperovskite Superionic Conductors Based on Cluster Ions. *Proc. Natl. Acad. Sci. U.S.A.* **2017**, *114*, 11046−11051.

(32) Mosconi, E.; Amat, A.; Nazeeruddin, M. K.; Gratzel, M.; Angelis, F. D. First-Principles Modeling of Mixed Halide Organometal Perovskites for Photovoltaic Applications. *J. Phys. Chem. C* **2013**, *117*, 13902−13913.

(33) Stoumpos, C. C.; Frazer, L.; Clark, D. J.; Kim, Y. S.; Rhim, S. H.; Freeman, A. J.; Ketterson, J. B.; Jang, J. L.; Kanatzidis, M. G. Hybrid Germanium Iodide Perovskite Semiconductors: Active Lone Pairs, Structural Distortions, Direct and Indirect Energy Gaps, and

https://doi.org/10.1021/acs.jpcc.2c03016
J. Phys. Chem. C 2022, 126, 13409−13415

Strong Nonlinear Optical Properties. *J. Am. Chem. Soc.* **2015**, *137*, 6804−6819.
(34) Swainson, I. P.; Hammond, R. P.; Soullière, C.; Knop, O.; Massa, W. Phase Transitions in the Perovskite Methylammonium Lead Bromide, $CH_3ND_3PbBr_3$. *J. Solid State Chem.* **2003**, *176*, 97−104.
(35) Yang, Z.; Rajagopal, A.; Chueh, C. C.; Jo, S. B.; Liu, B.; Zhao, T.; Jen, A. K.-Y. Stable Low-Bandgap Pb-Sn Binary Perovskites for Tandem Solar Cells. *Adv. Mater.* **2016**, *28*, 8990−8997.
(36) Fang, H.; Jena, P. Atomic-Level Design of Water-Resistant Hybrid Perovskites for Solar Cells by Using Cluster Ions. *J. Phys. Chem. Lett.* **2017**, *8*, 3726−3733.

https://doi.org/10.1021/acs.jpcc.2c03016
J. Phys. Chem. C 2022, 126, 13409−13415